Synthesis of Zr/La-BTC Bimetallic Metal-Organic Framework (MOF) for Oleic Acid Esterification

Agustino Zulys[1*], Adawiah Adawiah[2], Tiara Amalia Suminta[1], Iman Abdullah[1], Rizkha Fadhilla[3], Nasruddin Nasruddin[4], Takuya Mabuchi[5]

[1]Department of Chemistry, Faculty of Mathematics and Natural Sciences, University of Indonesia, Jl. Lingkar Kampus Raya, Pondok Cina, Beji, Depok, Jawa Barat 16424, Indonesia

[2]Integrated Laboratory Centre, Faculty of Science and Technology Universitas Islam Negeri Syarif Hidayatullah Jakarta, Jl. Ir. H. Juanda No. 95 Ciputat Tangerang Selatan 15412, Indonesia

[3]Department of Chemistry, Faculty of Science and Technology, Universitas Islam Negeri Syarif Hidayatullah Jakarta, Jl. Ir. H. Juanda No. 95 Ciputat Tangerang Selatan 15412, Indonesia

[4]Department of Mechanical Engineering, Faculty of Engineering, Universitas Indonesia, Kukusan, Beji, Depok, Jawa Barat 16425, Indonesia

[5]Frontier Research Institute of Interdiciplinary Sciences, Tohoku University, Japan

Email: zulys@ui.ac.id

Article Info

Abstract

Biodiesel plays an essential role in renewable energy as an alternative fuel to tackle the challenges of global warming, environmental degradation, and alternative fossil fuels. Oleic acid can be converted into biodiesel by the esterification process, which employs heterogeneous catalysts such as metal-organic frameworks (MOF). In this study, Zr/La-BTC MOFs were used as different kinds of catalysts to change oleic acid into biodiesel. The characterization results of Zr-BTC, La-BTC, and Zr/La-BTC using FTIR and XRD show that the MOF has been successfully formed. The crystallite sizes for La-BTC, and Zr/La-BTC MOFs are 15.7407 nm and 39.0392 nm, respectively. The surface area of Zr-BTC, La-BTC, and Zr/La-BTC MOFs are 167.101 m2/g, 12.328 m^2/g, and 4.764 m^2/g. The morphology of Zr-BTC MOF using SEM is irregular, La-BTC is rod-shaped crystal, and Zr/La-BTC is like a knot bond with a narrow waist. The most optimal reaction was obtained at a 5% (w/w) catalyst dosage of total oleic acid and methanol (1:60 mol), 65 °C, and a reaction time of 4 hours, producing 78.11% oleic acid conversion. GC-MS analysis identified that the biodiesel contains oleic acid, palmitic acid, methyl oleate, and methyl palmitate.

Keywords: Biodiesel; esterification; metal organic framework; oleic acid; Zr/La-BTC

1. INTRODUCTION

Biodiesel's biodegradability, low toxicity, high cetane number, and capacity to lower carbon dioxide emissions make it a viable replacement for fossil fuels. Biodiesel combustion produces significantly less pollution due to its elevated oxygen concentration as well as its reduced proportions of aromatic chemicals and sulfur [1]. Currently, biodiesel commercialization is hindered by the exorbitant expenses associated with feedstocks, including palm oil, sunflower oil, soybean oil, and rapeseed oil [2]. Utilizing inexpensive feedstocks, such as oleic acid, can increase the efficacy of biodiesel production [3]. Esterification reactions produce biodiesel from oleic acid [4–6]. On the other hand, the reversible reaction in esterification causes the biodiesel product to slowly form. As a result, a catalyst is required to accelerate the esterification kinetics [7].

Researchers are currently investigating and developing metalorganic frameworks (MOFs), which are catalysts with different properties, for biodiesel generation [6–10]. Metal–organic frameworks (MOFs) are crystalline structures with holes in them that are made up

of metal ions connected to organic molecules [11]. MOFs are different from other types of heterogeneous catalysts because they have a consistent pore structure, a large surface area, and active sites that are spread out. These characteristics enhance their catalytic properties [12]. 1,3,5-benzene tricarboxylic acid (H_3BTC) is a carboxylate-based organic ligand. Often used as a linker in MOF synthesis, it provides strong and stable MOF structures [13–15]. Li et al. used a hydrothermal method to make La-BTC, which was very stable and worked well as an electrochemical catalyst for reducing H_2O_2 in acidic conditions[16].

Lanthanum-based metal organic frameworks have been used by some researchers to break down dyes, turn glucose into 5-HMF, make hydrogen, and do the hydrogenation process[17–21]. On the other hand, researchers can use zirconium (Zr^{4+}) as an excellent hard Lewis acid for fatty acid esterification applications to construct MOFs. Using the solvothermal method, Larasati et al. produced Zr-BTC [22]. It was then used as a heterogeneous catalyst in the esterification reaction of palmitic acid into biodiesel. This reaction had the highest conversion rate of 69.20%. Constructing MOF in its bimetal form enhances its catalytic activity by providing a high number of active sites for each metal. In 2021, Adawiah et al. found that lanthanum and yttrium-based bimetallic MOFs with perylene linkers (La-Y-PYC) were more effective at photocatalysis than their single-metal counterparts (La-PTC and Y-PTC) [11].

The literature review indicates that no one has ever synthesized bimetallic MOFs based on zirconium and lanthanum metals with a 1,3,5-benzene tricarboxylic acid (H_3BTC) linker (Zr/La-BTC) and used it for the esterification of oleic acid into biodiesel. The goal of this study is to use the solvothermal method to make a bimetallic metal-organic framework (MOF) of Zr/La-BTC. We investigated the chemical characteristics and catalytic activity of MOF in the esterification of oleic acid during the biodiesel synthesis process.

2. RESEARCH METHODS
Materials
The materials used in this study were used without further purification. The materials were zirconium tetrachloride ($ZrCl_4$) (Sigma et al.), lanthanum nitrate hexahydrate ($La(NO_3)_3.6H_2O$) (Merck, p.a.), 1,3,5-benzene tricarboxylic acid (H_3BTC) (Merck, p.a.), N,N-dimethylformamide (DMF) (Merck, p.a.), methanol (Merck, p.a.), methanol (Merck, p.a.), distilled water, ethanol (Merck, p.a.), technical grade oleic acid (local), potassium hydroxide (Merck, p.a.), oxalic acid (Merck, p.a.), and phenolphthalein (pp) (Merck, p.a.).

Synthesis of MOF (Zr-BTC, La-BTC, and Zr/La-BTC)
$ZrCl_4$ (6 mmol) and H_3BTC (3 mmol) were dissolved in 60 mL of DMF and magnetically for 1 hour at 300 rpm. Then, the mixture was put into a Teflon-line autoclave and heated for 24 hours at 180 °C. Next, the mixture was centrifuged. The collected precipitate was washed with DMF and ethanol in amounts of 50 mL each. After that, the crystals were dried at 60 °C overnight. Finally, the synthesized Zr-BTC was activated at 200 °C for 2 hours.

A total of 2 mmol $La(NO_3)_3.6H_2O$ as a metal ion source and 2 mmol H_3BTC were dissolved in 5 mL of DMF and 50 mL of distilled water. Then, the mixture was stirred for 1 hour using a magnetic stirrer. The mixture was then put into a Teflon autoclave and heated at 220 °C for 24 hours. After that, the crystals were washed using DMF and methanol in as much as 50 mL each. Then, the La-BTC crystals were dried at 60 °C overnight. Finally, the synthesized La-BTC was activated at 200 °C for 2 hours.

$La(NO_3)_3.6H_2O$ (5.4 mmol), $ZrCl_4$ (0.6 mmol), and H_3BTC (3 mmol) were dissolved in 60 mL of DMF solution and stirred with a magnetic stirrer for 1 hour at 300 rpm. Then, the mixture was put into a Teflon-line autoclave and heated at 180 °C for 24 hours. After centrifugation and filtration, the precipitate was rinsed with 50 mL of DMF and ethanol. After that, the crystals were dried at 60 °C overnight. Finally, the synthesized Zr/La-BTC was activated at 200 °C for 2 hours.

The Characterization of MOF
MOFs were characterized using XRD (Rigaku Miniflex XRD) with Cu-K radiation ($\lambda = 1.5418$ Å) with a 2θ range of 3°–90° and a scan rate of 2°/min. The functional groups were determined using a FTIR spectrophotometer (Prestige 21 Spectrophotometer) in the wavenumber range 400–4000 cm^{-1} with a spectral resolution of 4 cm^{-1} by using KBr powder as the blank. SEM-EDX (Jeol Jsm 6510 La) at a voltage of 25 kV was used to investigate the morphology and distribution of the elements of MOF. The surface area, pore volume, and pore size of MOF were assessed using a surface area and porosity analyzer (Micromeritics Tristar II Plus Surface Area and Porosity Analyser) after a 3-hour degassing process at 150 °C.

Catalytic Activity Analysis of MOF
Zr-BTC, La-BTC, and Zr/La-BTC MOF of 1% (w/w) each of the total weight of oleic acid and methanol with a mole ratio of oleic acid: methanol (1:60) were put into a two-neck flask and then refluxed at 65 °C for 240 minutes. After that, the mixture was separated from the catalyst using centrifugation. Afterward, 4 mL of the solution was put into an Erlenmeyer, and a phenolphthalein indicator was added. Next, the mixture was titrated using 0.09 N KOH. The endpoint of the titration was reached when the solution changed color from colorless to pink, which was stable for 20 seconds. Furthermore, the percent conversion of fatty acids was calculated using Equation 1 [23]. For the standard solution,

4 mL of a mixture of oleic acid and methanol with a mole ratio of 1:60 was used. The analysis of the methyl ester components in the obtained biodiesel was investigated using a GC-MS instrument. The effect of catalyst dosage on the conversion of oleic acid was carried out using Zr/La-BTC dosages of 1, 3, and 5% (w/w). The kinetic analysis of oleic acid esterification was investigated using Zr/La-BTC 5% (w/w) with reaction times of 2, 3, 4, 6, and 8 hours.
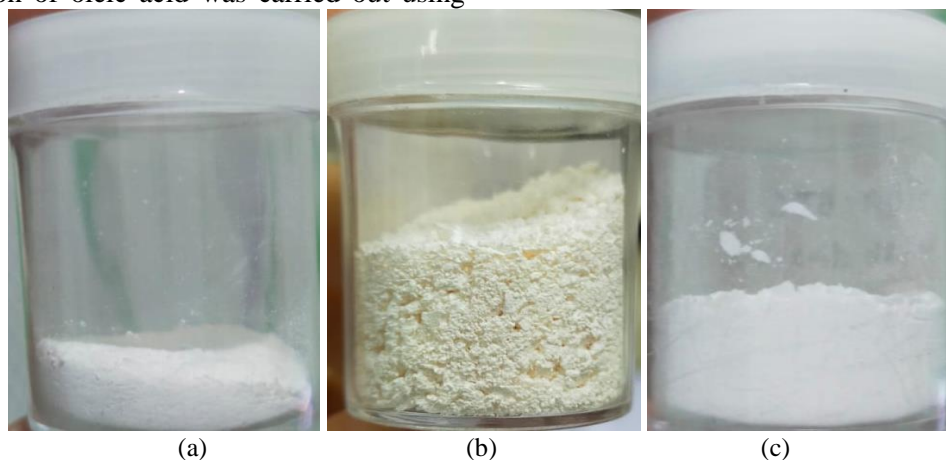

| (a) | (b) | (c) |

Figure 1. MOF Zr-BTC (a), La-BTC (b), and Zr/La-BTC MOF (c)

$$\% \text{ Conversion} = \left[1 - \frac{c_{KOH}}{c_{OA}} \times \left(\frac{V_{KOH}}{V_{sample}}\right)\right] \times 100 \quad \dots\dots (1)$$

Where C_{KOH} is the molar concentration of sodium hydroxide, C_{OA} is the molar concentration of oleic acid, V_{KOH} is the needed volume of sodium hydroxide solution to reach the end of titration, and V_{sample} is the volume of the sample collected in the reactor.

3. RESULTS AND DISCUSSION

We employed solvothermal methods to synthesize the Zr-BTC, La-BTC, and Zr/La-BTC metal-organic frameworks (MOFs). The solvothermal approach involves the crystallization of compounds from a solution at elevated temperatures and vapor pressures. This process facilitates the interaction between precursors in the solution during synthesis [24]. Solvothermal is the most popular method, allowing the system to work without requiring specific equipment. It also facilitates rapid crystal growth and results in high crystallinity [25]. Dimethylformamide (DMF) is a polar solvent that can dissolve many different types of chemicals, including BTC ligands [26]. It can't donate protons, though. The three MOFs produced exhibit distinct hues and textures, as depicted in Figure 1.

Characteristic of MOF

Figure 2 demonstrated a peak at 3195–3452 cm^{-1} that indicates the -OH strain vibrations originating from H$_2$O molecules trapped in all three MOFs. This peak differs from the BTC ligand at 2642–3195 cm^{-1}, which confirmed the -OH vibration of COOH. The observed band broadening suggests hydrogen bond formation between H$_2$O molecules trapped in the MOF. The band at 2758–2988 cm^{-1} is attributed to the C-H vibrations of aromatic groups. A significant band shift from 1712 cm^{-1}

$^{-1}$ on H$_3$BTC to 1632 cm^{-1} on each MOF was identified, suggesting that the MOF was successfully synthesized. The ligand and metal ion engage in a back-bonding interaction, which transfers electrons from the metal to the ligand until the metal becomes fully charged with electrons from the antibonding ligand. It causes a large shift. It reduces bond order, increases the distance between C=O bonds, and minimizes bond strength, requiring less energy to vibrate. The stretching vibration of the C-O group is at 1390 cm^{-1}, indicating the deprotonation of the carboxylate group of the H$_3$BTC ligand, which interacts with metal ions to create MOF. Furthermore, the absorption peak at 1562 cm^{-1} indicates the C=C bond in the aromatic ring, the peak around 752 cm^{-1} suggests out-of-plane CH deformation, the peak at 662 cm^{-1} demonstrates Zr-O stretching, and the peak at 512 cm^{-1} represents La-O stretch [27-28].
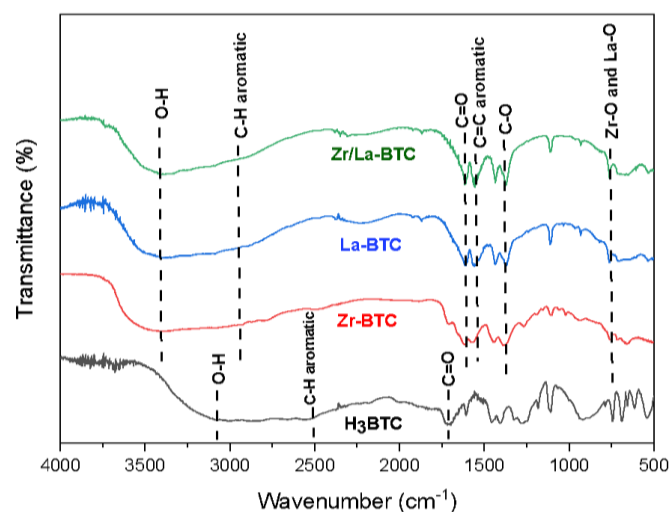

Figure 2. FTIR Spectra of H$_3$BTC, Zr-BTC, La-BTC, and Zr/La-BTC

Figure 3 depicts the diffraction patterns of the prepared three MOFs. The Zr-BTC MOF exhibits fewer sharp diffraction peaks, indicating that the obtained Zr-BTC MOF is amorphous (Figure 3a). The Zr-BTC MOF presented two unique diffraction peaks at 8.26° and 8.63°, indicating that the Zr-BTC MOF had been successfully formed due to the similarity of the diffraction peaks with the standard Zr-BTC (CCDC 1002672). The large peak at 27° indicates the formation of zirconium oxide (ZrO_2). Figure 3b demonstrates the
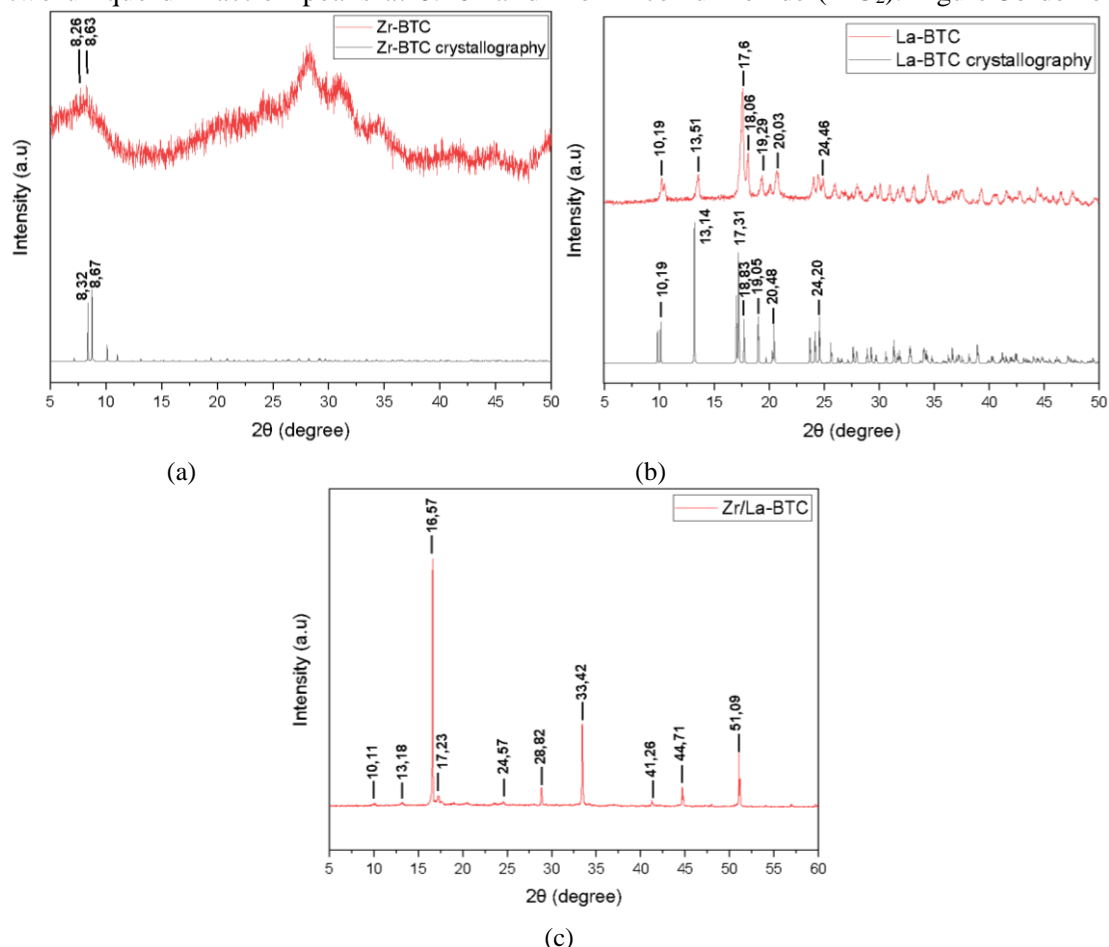

(a)

(b)

(c)

Figure 3. Diffraction pattern of (a) Zr-BTC, (b) La-BTC, and (c) Zr/La-BTC

sharp diffraction peaks of La-BTC, confirming its crystal structure. The diffraction pattern of La-BTC MOF consists of peaks at 2θ = 10.19°, 13.51°, 17.6°, 18.06°, 19.29°, 20.03°, and 24.46°. The diffraction peaks corresponding to La-BTC are 10.19°, 13.14°, 17.31°, 18.83°, 19.05°, 20.48°, and 24.20° (CCDC 290771). The diffraction pattern of the Zr/La-BTC MOF shows strong diffraction peaks, indicating that Zr/La-BTC is crystalline (Figure 3c). The diffraction pattern of Zr/La-BTC MOF is similar to that of standard La/Zr-BTC MOF (JCPDS No. 27-1704). The diffraction peaks of Zr/La-BTC were found at 2θ = 10.11°, 13.18°, 16.57°, 17.23°, and 24.57° (JCPDS No. 27-1704). This suggests the successful synthesis of La-BTC and Zr/La-BTC.

Zr-BTC exhibits an irregular morphology (irregular form) (Figure 4a–b). Previous research has revealed that Zr-BTC has an irregular form and an inhomogeneous size [22,29]. La-BTC MOF possesses a rod-like crystalline morphology (Figure 4c–d). It builds on the previous research [17,31]. Meanwhile, the Zr/La-BTC bimetallic MOF has a rod-like shape with a small waist, similar to the previous research [31] (Figure 4e-f). When comparing the morphology of Zr/La-BTC to that of La-BTC, it becomes evident that the La/Zr ratio in Zr/La-BTC significantly influences the resulting structure. La-BTC exhibits a rod-like shape, while Zr-BTC consists of amorphous particles with irregular morphology. The doping of Zr species in the La-BTC matrix can significantly alter the original structure, necessitating the use of a suitable quantity of doping. Utilizing too many Zr species in La-BTC will prevent the formation of a dense crystal structure and collapse the knot bonding system [30].
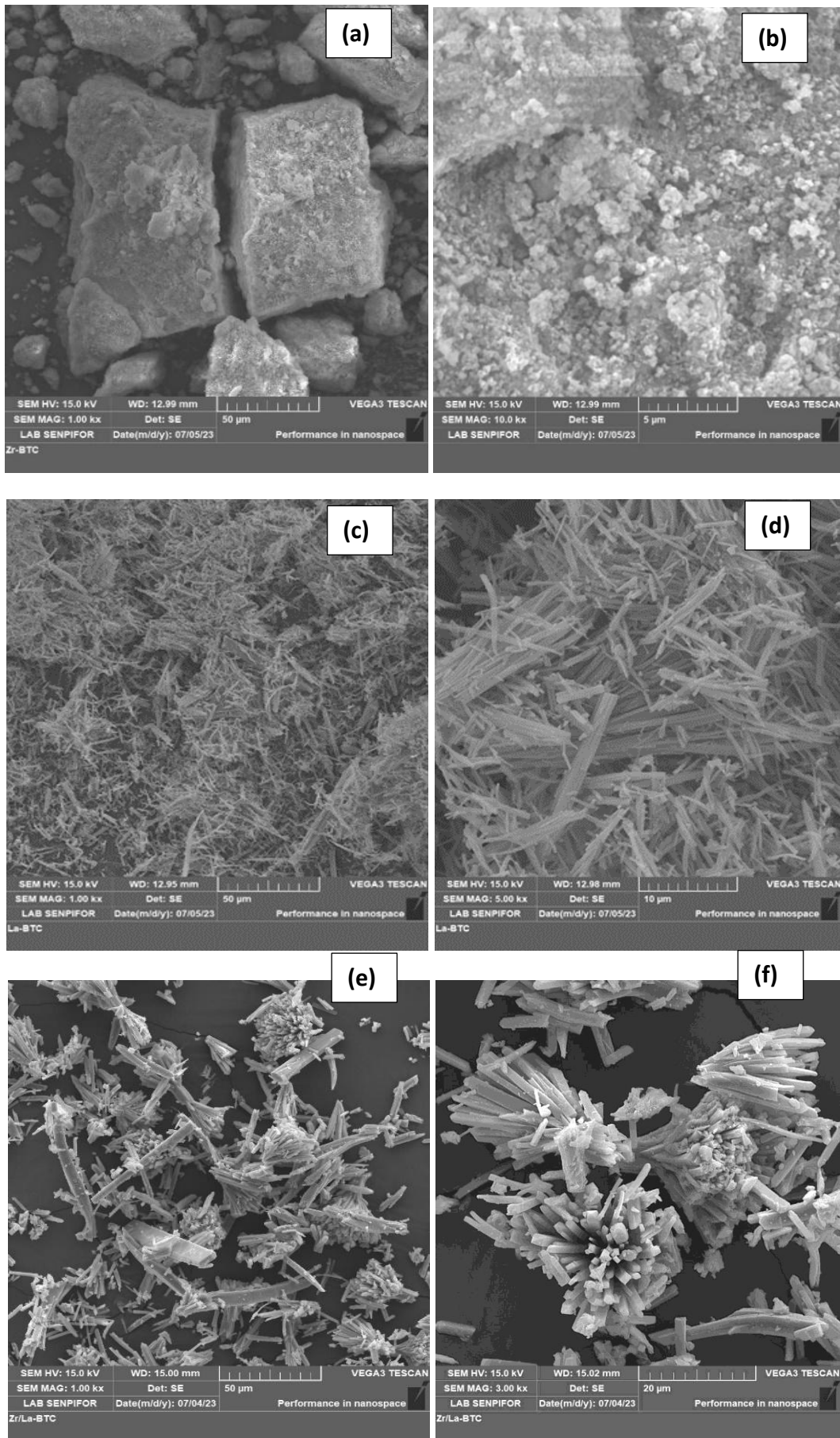
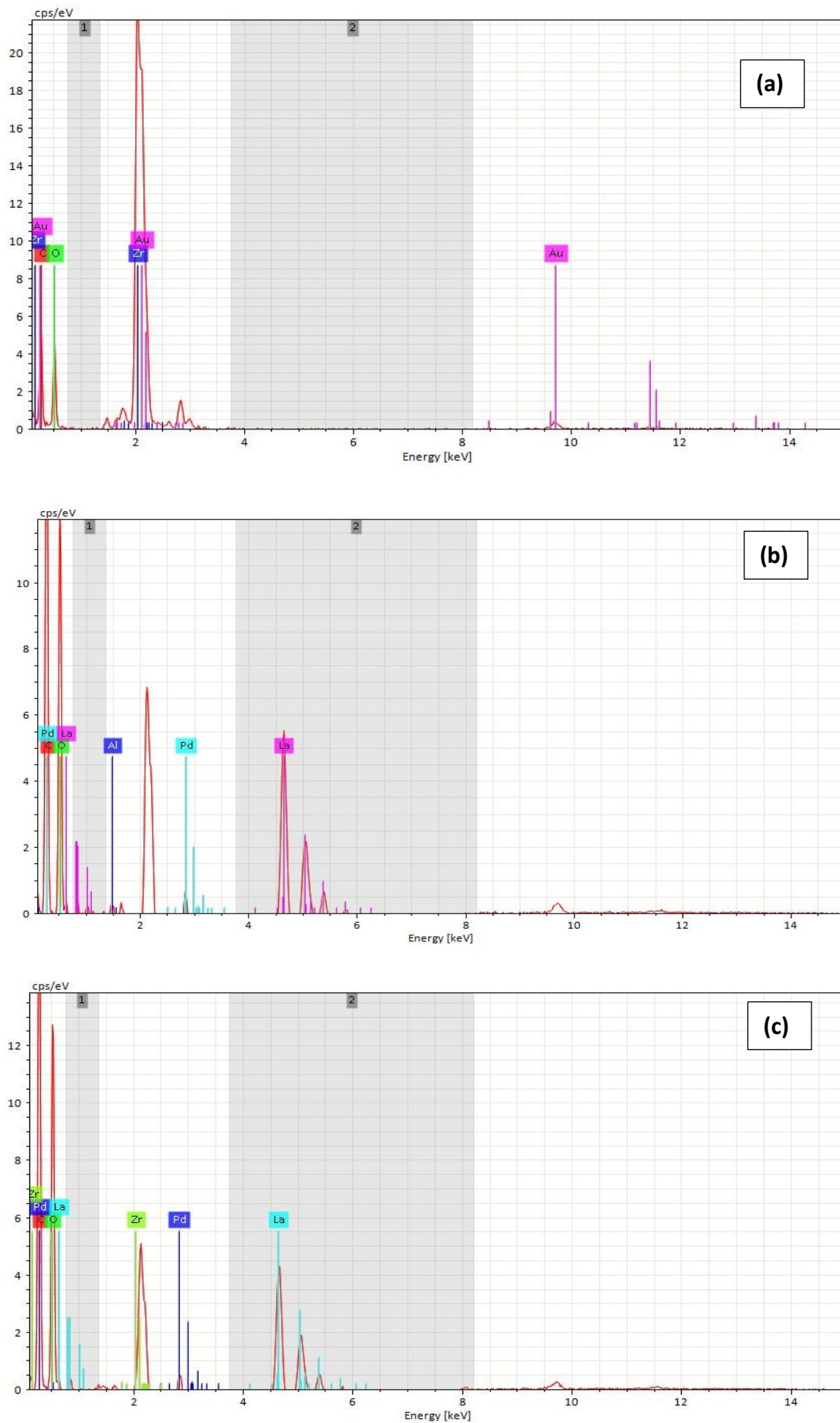**Figure 4.** The morphology of Zr-BTC (a-b); La-BTC (c-d)); and Zr/La-BTC (e-f)

Figure 5. The EDX spectrum of Zr-BTC (a); La-BTC (b); and Zr/La-BTC (c)

Table 1. Element composition of Zr-BTC, La-BTC, and Zr/La-BTC

Element	Element composition (%)		
	MOF Zr-BTC	**MOF La-BTC**	**MOF Zr/La-BTC**
C	58.91	57.31	56.98
O	24.94	35.82	31.83
Zr	16.15		2.86
La		6.34	8.33
Al		0.53	

The composition of the elements in the ferrites obtained from EDX is shown in Figure 5 and Table 1. The EDX spectrum shows the presence of other elements like Al and Pd elements in Zr-BTC and La/Zr-BTC MOF. It indicated the impurities of Zr-BTC and La/Zr-BTC.

The Zr-BTC MOF has a surface area of 167.101 m^2/g. Because Zr-BTC is amorphous, the particle size is smaller, resulting in a larger surface area. The surface area of La-BTC is 12.328 m^2/g, whereas that of Zr/La-BTC is 4.764 m^2/g. The surface area represents the rising trend of average pore diameter and cumulative pore volume, with the larger the surface area, the larger the pore diameter and pore volume. The average pore diameters for Zr-BTC, La-BTC, and Zr/La-BTC were 94.943 Å, 38.008 Å, and 38.031 Å, respectively. For Zr-BTC, La-BTC, and Zr/La-BTC, the cumulative pore volumes were 1.567 cc/g, 0.032 cc/g, and 0.011 cc/g, respectively. The addition of Zr to La-BTC decreased the surface area of Zr/La-BTC by decreasing pore volume and increasing particle size.

Catalytic Activity of MOF

We employed Zr-BTC, La-BTC, and Zr/La-BTC MOFs as catalysts in the esterification of biodiesel using oleic acid as a substrate. The objective was to determine the most effective catalyst for the reaction. To prevent a potential reverse reaction caused by the water byproduct, it is crucial to promptly titrate the product. The combination of water and methyl oleate undergoes a chemical reaction resulting in the formation of oleic acid.
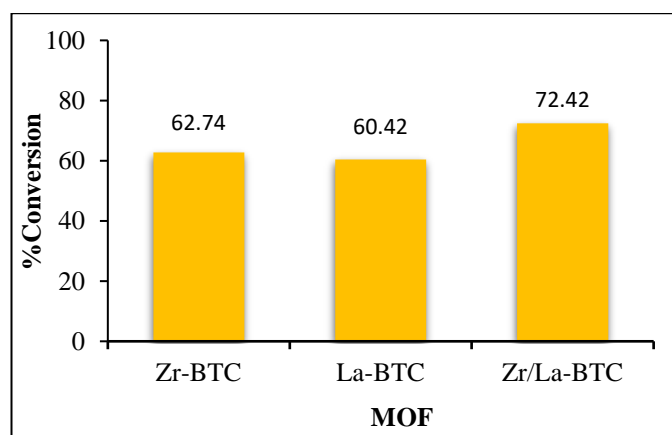

Figure 6. The Conversion of oleic acid of La-BTC, Zr-BTC, and Zr/La-BTC

Acid catalysts are usually applied to esterification reactions to increase the reaction rate and act as dehydrating agents. The acidity of the catalyst has a significant effect on the esterification reaction. The stronger the acidity of the catalyst, the greater the percent conversion of fatty acids into esters. Arbain and Salimon stated that perchloric acid gives a higher percent yield of TMP esters compared to sulfuric acid, p-toluenesulfonic acid, hydrochloric acid, and nitric acid because it is one of the strongest Brønsted-Lowry acids with a pKa value of -10^{20} [31].

The percentage conversion of oleic acid to methyl oleate using Zr-BTC, La-BTC, and Zr/La-BTC catalysts were 62.7368%, 60.4210%, and 72.4210%, respectively (Figure 6). The La/Zr-BTC bimetallic MOF yielded an increase in oleic acid conversion percent compared to the La-BTC and Zr-BTC monotallic MOFs. The higher percent conversion was influenced by the increased acidity of Zr/La-BTC MOF due to the presence of two types of acidic metals Zr and La [32]. Kumaresan et al. stated that doping metal ions such as lanthanum, zirconium and cerium into the mesoporous TiO$_2$ framework can increase acidity, which leads to better catalytic behavior [33]. Salunke and Yadav also reported that the total acidity of zirconium increased from pure zirconium to Zr$_4$La$_1$ when lanthanum was added with a total acidity of 0.24 and 0.42, respectively[34].

On the other hand, Zr-BTC MOF has a higher surface area compared to La-BTC and Zr/La-BTC compounds. The catalytic activity of a material generally increases as the surface area, pore size, and pore volume increase. However, this study presents contrary findings between the surface area and the observed catalytic activity. This is because not all active sites on the catalyst participate in the catalysis reaction. Therefore, the catalytic activity of these three MOFs is likely to be predominantly determined by the Lewis acidic strength of the MOFs. The study demonstrated that Zr metal, with its 4+ charge, outperforms La metal in acidity. Therefore, the percent conversion of oleic acid by Zr-BTC was slightly higher than that of La-BTC.

Additionally, a material's crystal structure closely influences its catalytic activity [35-36]. Increasing crystallinity will increase the catalyst's stability and reduce the reaction's activation energy. A crystalline catalyst provided better activity than the amorphous catalysts. Wang et al. said that crystalline tungsten oxide

formed on the titania surface and was better at water stability and removing NOX at temperatures below 250 °C than amorphous tungsten oxide. Compared to Zr-BTC, La-BTC and Zr/La-BTC have higher crystallinity. As a result, La-BTC and Zr/La-BTC have a higher catalytic activity for converting oleic acid [37].
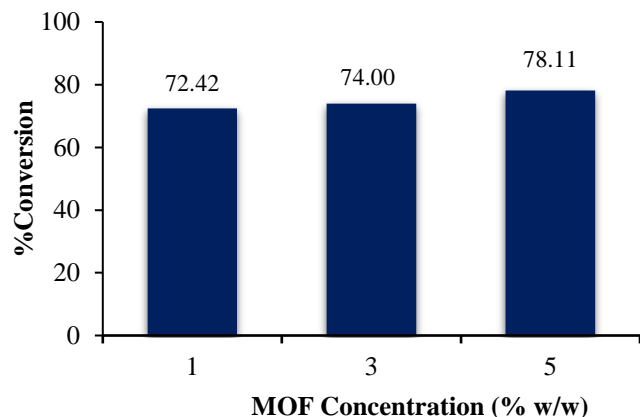

Figure 7. Effect of catalyst dosage on the conversion of oleic acid

Figure 7 shows the percentage of oleic acid converted to methyl oleate. At 1%, 3%, and 5% (w/w), the La/Zr-BTC dosages were 72.42%, 74%, and 78.11%, respectively. Figure 7 illustrates how well a 5% Zr/La-BTC catalyst converted oleic acid to methyl oleate. According to Senoymak & Ilgen, the catalyst and the precursor interact more easily when the number of MOF active sites increases, resulting in a higher conversion of oleic acid [38].

Figure 8 shows an analogy between the reaction mechanism of fatty acid esterification and methanol using a MOF-based catalyst [39]. When we use a MOF catalyst, we initiate the reaction by protonating oxygen (O) on carboxylic acid with Zr or La on the MOF. Furthermore, other Zr or La atoms on the MOF, which are positively charged and capable of capturing electron pairs, will protonate the O atom on the methanol. Then, as nucleophiles, methoxy will bind with C-carbonyl on carboxylic acids. The resulting leaving group is H_2O, which is a byproduct of this reaction. Furthermore, this reaction deprotonates the methyl ester (biodiesel), producing a neutrally charged catalyst. The entire chemical reaction produces methyl ester (biodiesel), water (H_2O), and a catalyst.

The biodiesel contains methyl oleate, methyl palmitate, oleic acid, and palmitic acid. It shows that the Zr/La-BTC catalyst can effectively change oleic acid into methyl oleate, which is biodiesel. We identified the presence of methyl palmitate in this reaction because we used technical-grade oleic acid, which had a low concentration of palmitic acid. Furthermore, because the conversion rate of oleic acid was only 78.11%, the biodiesel contained both oleic acid and palmitic acid.
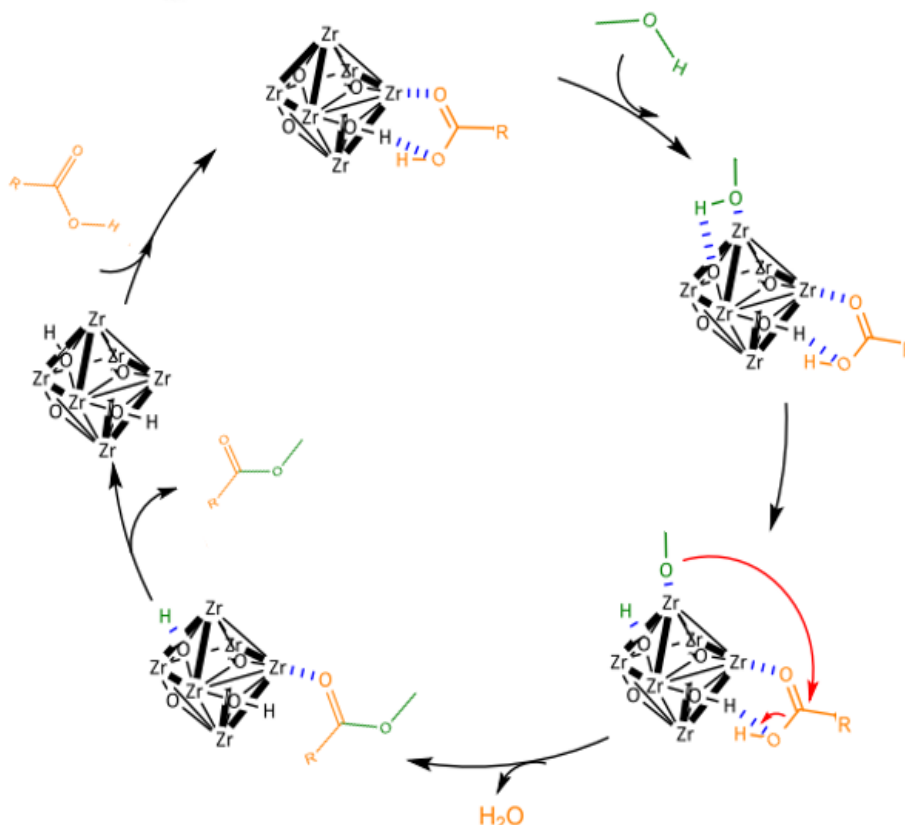

Figure 8. The possible reaction mechanism of oleic acid and methanol using Zr-MOF-based Catalysts

4. CONCLUSIONS

This study has successfully synthesized bimetal metal organic framework materials based on lanthanum and zirconium metals with benzene tricaborksilic acid organic linker. The obtained Zr/La-BTC bimetallic MOF showed higher catalytic activity in the esterification reaction of oleic acid to biodiesel than its monometal MOFs, namely Zr-BTC and La-BTC. The Zr/La-BTC MOF provided the most optimum catalytic activity at 65°C, 5% (w/w) MOF mass and 4 hours reaction time with a percent conversion of 78.11%. This research provides the most updated insights on the development of bimetal MOF-based catalysts for esterification reaction applications in biodiesel production.

ACKNOWLEDGMENTS

REFERENCES

1. Basumatary SF, Patir K, Das B, et al. Production of renewable biodiesel using metal organic frameworks based materials as efficient heterogeneous catalysts. *J Clean Prod*. 2022;358:131955. doi:10.1016/j.jclepro.2022.131955

2. Kusmiyati K. Reaksi katalitis esterifikasi asam oleat dan metanol menjadi biodiesel dengan metode distilasi reaktif. *Reaktor*, 2008; 12(2), 78-82. https://doi.org/10.14710/reaktor.12.2.78-82.

3. Zhang Y, Wong WT, Yung KF. Biodiesel production via esterification of oleic acid catalyzed by chlorosulfonic acid modified zirconia. *Applied Energy*, 2014; *116*, 191–198. https://doi.org/10.1016/j.apenergy.2013.11.044

4. Zhou K, Chaemchuen S. Metal-Organic Framework as Catalyst in Esterification of Oleic Acid for Biodiesel Production. *International Journal of Environmental Science and Development*. 2017;8(4):251-254. doi:10.18178/ijesd.2017.8.4.957

5. Moradi P, Saidi M, Najafabadi AT. Biodiesel production via esterification of oleic acid as a representative of free fatty acid using electrolysis technique as a novel approach: Non-catalytic and catalytic conversion. *Process Safety and Environmental Protection*. 2021;147:684-692. doi:10.1016/j.psep.2020.12.032

6. Dechakhumwat S, Hongmanorom P, Thunyaratchatanon C, Smith SM, Boonyuen S, Luengnaruemitchai A. Catalytic activity of heterogeneous acid catalysts derived from corncob in the esterification of oleic acid with methanol. *Renew Energy*. 2020;148:897-906. doi:10.1016/j.renene.2019.10.174

7. Aziz I, Nurbayti S, Ulum B. Esterifikasi Asam Lemak Bebas Dari Minyak Goreng Bekas. *Jurnal Kimia VALENSI*. 2011;2(2). doi:10.15408/jkv.v2i2.201

8. Zhang Q, Yang X, Yao J, Cheng J. Bimetallic MOF-Derived Synthesis of Cobalt-Cerium Oxide Supported Phosphotungstic Acid Composites for the Oleic Acid Esterification. *J Chem*. 2021;2021:1-9. doi:10.1155/2021/2131960

9. Zhang Q, Wang J, Zhang S, Ma J, Cheng J, Zhang Y. Zr-Based Metal-Organic Frameworks for Green Biodiesel Synthesis: A Minireview. *Bioengineering*. 2022;9(11):700. doi:10.3390/bioengineering9110700

10. Taddeo F, Vitiello R, Russo V, Tesser R, Turco R, Di Serio M. Biodiesel Production from Waste Oil Catalysed by Metal-Organic Framework (MOF-5): Insights on Activity and Mechanism. *Catalysts*. 2023;13(3):503. doi:10.3390/catal13030503

11. Adawiah A, Yudhi MDL, Zulys A. Photocatalytic Degradation of Methylene Blue and Methyl Orange by Y-PTC Metal-Organic Framework. *Jurnal Kimia Valensi*. 2021;7(2):129-141. doi:10.15408/jkv.v7i2.22267

12. Wen Y, Zhang J, Xu Q, Wu XT, Zhu QL. Pore surface engineering of metal–organic frameworks for heterogeneous catalysis. *Coord Chem Rev*. 2018;376:248-276. doi:10.1016/j.ccr.2018.08.012

13. Jiang Z, Chen Y, Xing M, Ji P, Feng W. Fabrication of a Fibrous Metal–Organic Framework and Simultaneous Immobilization of Enzymes. *ACS Omega*. 2020;5(36):22708-22718. doi:10.1021/acsomega.0c00868

14. Lestari WW, Inayah WC, Rahmawati F, Larasati L, Purwanto A. Metal-Organic Frameworks Based on Zinc(II) and Benzene-1,3,5-Tricarboxylate Modified Graphite: Fabrication and Application as an Anode Material in Lithium-Ion Batteries. *Journal of Mathematical and Fundamental Sciences*. 2020;52(1):81-97. doi:10.5614/j.math.fund.sci.2020.52.1.6

15. Mylonas-Margaritis I, Mayans J, McArdle P, Papatriantafyllopoulou C. ZnII and CuII-Based Coordination Polymers and Metal Organic Frameworks by the of Use of 2-Pyridyl Oximes and 1,3,5-Benzenetricarboxylic Acid. *Molecules*. 2021;26(2):491. doi:10.3390/molecules26020491

16. Li Y, Zhong Y, Huang J. The synthesis of a lanthanum metal–organic framework and its sensitivity electrochemical detection of H_2O_2. *Chemical Papers*. 2017;71(5):913-920. doi:10.1007/s11696-016-0011-9

17. Riezzati N, Krisnandi YK, Zulys A. Metal organic frameworks of lanthanum and iron using BDC linker as catalysts for glucose conversion into 5-hydroxymethylfurfural (5-HMF). *IOP Conf Ser Mater Sci Eng*. 2020;902(1):012044. doi:10.1088/1757-899X/902/1/012044

18. Buhori A, Zulys A, Gunlazuardi J. Synthesis of Lanthanum metal-organic frameworks (La-MOFs) as degradation photocatalyst of Rhodamine-B. In: ; 2020:040033. doi:10.1063/5.0013010

19. Zulys A, Adawiah A, Gunlazuardi J, Yudhi MDL. Light-Harvesting Metal-Organic Frameworks (MOFs) La-PTC for Photocatalytic Dyes Degradation. *Bulletin of Chemical Reaction Engineering & Catalysis*. 2021;16(1):170-178. doi:10.9767/bcrec.16.1.10309.170-178

20. Batubara NH, Zulys A. Synthesis, Structural, Spectroscopic, and Morphology of Metal-Organic Frameworks Based on La (III) and Ligand 2,6-Napthalenedicarboxylic acid (La-MOFs) for Hydrogen Production. *IOP Conf Ser Mater Sci Eng*. 2019;546(4):042005. doi:10.1088/1757-899X/546/4/042005

21. Tshuma P, Makhubela BCE, Öhrström L, et al. Cyclometalation of lanthanum(<scp>iii</scp>) based MOF for catalytic hydrogenation of carbon dioxide to formate. *RSC Adv*. 2020;10(6):3593-3605. doi:10.1039/C9RA09938G

22. Larasati I, Winarni D, Putri FR, Hanif QA, Lestari WW. Synthesis of Metal-organic Frameworks Based on Zr^{4+} and Benzene 1,3,5-Tricarboxylate Linker as Heterogeneous Catalyst in the Esterification Reaction of Palmitic Acid. *IOP Conf Ser Mater Sci Eng*. 2017;214:012006. doi:10.1088/1757-899X/214/1/012006

23. Deus MS, Deus KCO, Lira DS, Oliveira JA, Padilha CEA, Souza DFS. Esterification of Oleic Acid for Biodiesel Production Using a Semibatch Atomization Apparatus. *International Journal of Chemical Engineering*. 2023;2023:1-14. doi:10.1155/2023/6957812

24. González CMO, Morales EMC, Tellez A de MN, Quezada TES, Kharissova O V., Méndez-Rojas MA. CO2 capture by MOFs. In: *Handbook of Greener Synthesis of Nanomaterials and Compounds*. Elsevier; 2021:407-448. doi:10.1016/B978-0-12-822446-5.00018-6

25. McKinstry C, Cathcart RJ, Cussen EJ, Fletcher AJ, Patwardhan S V., Sefcik J. Scalable continuous solvothermal synthesis of metal organic framework (MOF-5) crystals. *Chemical Engineering Journal*. 2016;285:718-725. doi:10.1016/j.cej.2015.10.023

26. Heravi MM, Ghavidel M, Mohammadkhani L. Beyond a solvent: triple roles of dimethylformamide in organic chemistry. *RSC Adv*. 2018;8(49):27832-27862. doi:10.1039/C8RA04985H

27. Milakin KA, Gupta S, Kobera L, et al. Effect of a Zr-Based Metal–Organic Framework Structure on the Properties of Its Composite with Polyaniline. *ACS Appl Mater Interfaces*. 2023;15(19):23813-23823. doi:10.1021/acsami.3c03870

28. Adawiah A, Gunawan MS, Aziz I, Oktavia W. Synthesis of Bimetallic Metal-Organic Frameworks (MOFs) La-Y-PTC for Enhanced Dyes Photocatalytic Degradation. *Bulletin of Chemical Reaction Engineering & Catalysis*. 2023;18(1):118-130. doi:10.9767/bcrec.16130

29. Lestari WW, Suharbiansah RSR, Larasati L, et al. A zirconium(IV)-based metal–organic framework modified with ruthenium and palladium nanoparticles: synthesis and catalytic performance for selective hydrogenation of furfural to furfuryl alcohol. *Chemical Papers*. 2022;76(8):4719-4731. doi:10.1007/s11696-022-02193-1

30. Kong L, Zhang J, Wang Y, et al. Bowknot-like Zr/La bimetallic organic frameworks for enhanced arsenate and phosphate removal: Combined experimental and DFT studies. *J Colloid Interface Sci*. 2022;614:47-57. doi:10.1016/j.jcis.2022.01.033

31. Arbain NH, Salimon J. The Effects of Various Acid Catalyst on the Esterification of Jatropha Curcas Oil based Trimethylolpropane Ester as Biolubricant Base Stock. *E-Journal of Chemistry*. 2011;8(s1):S33-S40. doi:10.1155/2011/789374

32. Kumari A, Kaushal S, Singh PP. Bimetallic metal organic frameworks heterogeneous catalysts: Design, construction, and applications. *Mater Today Energy*. 2021;20:100667. doi:10.1016/j.mtener.2021.100667

33. Kumaresan L, Prabhu A, Palanichamy M, Arumugam E, Murugesan V. Synthesis and characterization of Zr^{4+}, La^{3+} and Ce^{3+} doped mesoporous TiO_2: Evaluation of their photocatalytic activity. *J Hazard Mater*. 2011;186(2-3):1183-1192. doi:10.1016/j.jhazmat.2010.11.124

34. Salunke JY, Yadav GD. Lanthanum doped zirconia as an efficient catalyst for reductive amination of 2-methoxybenzaldehyde with dimethylformamide via Leuckart type reaction. *ES Materials & Manufacturing*. Published online 2023. doi:10.30919/esmm5f853

35. Xu L, Yang Q, Hu L, et al. Insights over Titanium Modified FeMgOx Catalysts for Selective Catalytic Reduction of NOx with NH3: Influence of Precursors and Crystalline Structures. *Catalysts*. 2019;9(6):560. doi:10.3390/catal9060560

36. Yu L, Zhong Q, Deng Z, Zhang S. Enhanced NOx removal performance of amorphous Ce-Ti catalyst by hydrogen pretreatment. *J Mol Catal A Chem*. 2016;423:371-378. doi:10.1016/j.molcata.2016.07.040

37. Wang C, Yang S, Chang H, Peng Y, Li J. Dispersion of tungsten oxide on SCR performance of $V_2O_5WO_3/TiO_2$: Acidity, surface species and catalytic activity. *Chemical Engineering Journal*. 2013;225:520-527. doi:10.1016/j.cej.2013.04.005

38. Senoymak Tarakcı MI, Ilgen O. Esterification of Oleic Acid with Methanol Using $Zr(SO_4)_2$ as a Heterogeneous Catalyst. *Chem Eng Technol*. 2018;41(4):845-852. doi:10.1002/ceat.201700254

39. Villoria-del-Álamo B, Rojas-Buzo S, García-García P, Corma. Zr-MOF-808 as catalyst for amide esterification. *Chem. Eur. J*. 2021, 27, 4588. https://doi.org/10.1002/chem.202003752